small
NANO MICRO

3D Nanofabrication of Fluidic Components by Corner Lithography

*Erwin J. W. Berenschot, Narges Burouni, Bart Schurink, Joost W. van Honschoten, Remco G. P. Sanders, Roman Truckenmuller, Henri V. Jansen, Miko C. Elwenspoek, Aart A. van Apeldoorn, and Niels R. Tas**

Dr. Joost W. van Honschoten is deceased, as of January 12th, 2011.

A *reproducible wafer-scale method to obtain 3D nanostructures is investigated. This method, called corner lithography, explores the conformal deposition and the subsequent timed isotropic etching of a thin film in a 3D shaped silicon template. The technique leaves a residue of the thin film in sharp concave corners which can be used as structural material or as an inversion mask in subsequent steps. The potential of corner lithography is studied by fabrication of functional 3D microfluidic components, in particular i) novel tips containing nano-apertures at or near the apex for AFM-based liquid deposition devices, and ii) a novel particle or cell trapping device using an array of nanowire frames. The use of these arrays of nanowire cages for capturing single primary bovine chondrocytes by a droplet seeding method is successfully demonstrated, and changes in phenotype are observed over time, while retaining them in a well-defined pattern and 3D microenvironment in a flat array.*

1. Introduction

The advent of microelectronics in the 1960's has resulted in a multitude of electronic but also mechanical and fluidic micro-components. The functionality of micro and nanostructures can be greatly enhanced if nano-patterning techniques can be applied to non-planar objects and at surfaces that are arbitrarily oriented in space. An example of such a technique is focused ion beam (FIB) milling[1] in which the focused ion beam can be applied to any spot on a 3D micro-object. However, when large numbers of objects have to be machined, the disadvantage of this technique is the intrinsic serial nature. Corner lithography[2–4] is a wafer scale nano-patterning technique that has the interesting property that it forms nanostructures in sharp concave corners, independent of their orientation in space. This is a consequence of the isotropic nature of the two basic steps involved: conformal deposition followed by isotropic etching. **Figure 1** illustrates the principle of corner lithography at the intersection of two planes. After conformal deposition of a layer of thickness t the effective thickness in the corner is $a = t/\sin(\alpha/2)$, where α is the angle of the concave corner. After isotropic thinning by an amount of r the remaining material in the corner will have a thickness $b = a - r$.[2] If the corner is formed by the intersection of two planes the resulting material will constitute a nanowire, if the corner is formed by the intersection of three or more planes a nano-dot will be formed, possibly connected to a frame of nanowires formed in the corners between intersecting pairs of planes.

E. J. W. Berenschot, N. Burouni,
Dr. J. W. van Honschoten, R. G. P. Sanders,
Dr. H. V. Jansen, Prof. M. C. Elwenspoek, Dr. N. R. Tas
Transducers Science and Technology Group
MESA+ Institute for Nanotechnology
University of Twente
P. O. Box 217, 7500 AE Enschede, The Netherlands
E-mail: N.R.Tas@utwente.nl

B. Schurink, Dr. R. Truckenmuller, Dr. A. A. van Apeldoorn
Tissue Regeneration Group, MIRA Institute
for Biomedical Technology and Technical Medicine
University of Twente
P. O. Box 217, 7500 AE Enschede, The Netherlands

DOI: 10.1002/smll.201201446

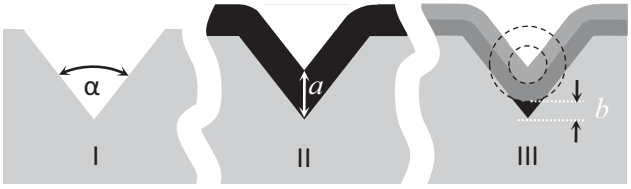

Figure 1. Corner Lithography concept (cross-sectional view): (I) V-groove template preparation, angle α (II) deposition of conformal material, layer thickness *t* and thickness *a* in the corner (III) time controlled selective isotropic thinning by distance *r* leaving a nano feature of height *b*.

Corner lithography was initially developed in our lab by Sarajlic et al.[2] who created a silicon nitride nanowire pyramid. Berenschot et al.[3] investigated the use of structures formed by corner lithography as a mask material in subsequent steps. Yu et al.[4] independently developed corner lithography and applied it for the fabrication of nano-ring particles and photonic crystals.

In the current work, we introduce the fabrication of nano-apertures by corner lithography, and show the integration of corner lithography based structures in microfluidic devices. The basic functionality of these devices is demonstrated. In the most advanced application, we show the feasibility of using these structures to separate individual primary chondrocytes in 2D while maintaining their 3D spherical morphology.

Corner lithography can be used as a wafer scale method for obtaining apertures at the apex of micro-pyramids, or near the apex of these pyramids ("side-apertures"). These modified pyramids can be applied as functional tips in Atomic Force Microscopy (AFM) based liquid deposition techniques, such as dip-pen nanolithography (DPN),[5] Nano-Scale Dispensing (NADIS),[6–8] and fountain pen based lithography.[9,10] An emerging application of fluidic AFM is in single cell biological or biophysical experiments.[11] Pyramids containing nano-apertures could find application as advanced electrospray emitters for the generation of nano-scale droplets.[12] In a wider perspective, well-defined nano-apertures can be applied in DNA translocation experiments,[13–16] and in nano-filter devices.[17–19]

In addition, we used the parallel nature of corner lithography to create arrays of silicon nitride nanowire pyramids in a perforated membrane to form a single cell trapping device. By using these flat arrays of pyramids, cells can be distributed in a predefined pattern while preserving their natural 3D morphology. An ultimate cell culture device is created by melting a glass tube on top of these arrays.[20,21] These pyramid arrays were then used for capturing single chondrocytes, capturing each individual cell in one single pyramid. We observed that trapped cells maintained their initial rounded morphology and an increasing amount of filopodia-like structures were protruding from these entrapped cells during the first days after cell seeding. This proofs that these cells were metabolically active. Based on the aforementioned results we show that by corner lithography one can not only batch-wise produce functional AFM tips, but also a platform to study single cells *in vitro* in a 2D array of nanowire pyramids, in which they maintain their three dimensional phenotype.

1.1. Control of Meniscus Size in AFM-Based Deposition

A crucial issue in all AFM based deposition processes is control over and reduction of the lines or dots written. This is closely related to the size of the meniscus formed at the tip-substrate contact spot.[5] However, this is not the only factor. Also the dependence of the surface diffusion on relative humidity (RH) plays an important role.[22]

In fountain pen lithography[9,10] and NADIS,[6–8] a local environment with a high vapor pressure is formed by the supply of ink, or a bulk liquid flow is supplied all the way to the apex. In both processes, limiting the size of the meniscus formed by guiding the ink through a nano-structured tip can be beneficial for the control of the resolution. This is the rationale behind creating side-apertures near the apex of the pyramidal tip (section 2.1). In the NADIS process, a droplet of ink is deposited in the back of the hollow pyramidal tip. Liquid is transferred to the substrate through a hole at the apex of the pyramid, which is commonly machined by FIB. Machining the aperture in a wafer-scale process would be desirable because it provides many more probes at much lower cost. Potentially it also increases the reproducibility of the aperture size. The aperture size plays a crucial role in the deposited feature size.[8] In Section 2.1 we introduce a wafer-scale procedure to fabricate a nano-aperture at the tip apex.

1.2. Cell Trapping Devices

Cell trapping is a crucial step in many innovative biological experiments like electroporation, patch clamping, and drug injection.[23] The main trapping mechanisms reported are mechanical and di-electrophoretic (DEP) trapping.[23] Mechanical traps include weir-type filters,[24,25] pillar based filters,[26] and perforated membrane based filters.[27] A common feature of these traps is that the cells are captured in a relative closed environment, which may influence their properties. An indication of this is given by Randall et al.,[28] who created 3D microwell arrays for cell culture. They showed that perforating the walls of the 3D wells increases cell viability as well as insulin secretion of β-cells in response to a glucose stimulus. While Randall et al. created 3D wells for clusters of cells, in the current work we focus on 3D open traps for single cells based on nanowire pyramidal structures (Section 2.2).

2. Results and discussion

2.1. Nano-Apertures Near or at the Apex of a Micro-Pyramid

In this section we present two nano-fabrication procedures: one to form an aperture at the apex of a micro pyramid, and one to form side-apertures near the apex of the pyramid. The first procedure focuses on the fabrication of the nano-aperture

small 2012,
DOI: 10.1002/smll.201201446

NANO MICRO small

only, and is illustrative for the formation of a nano-structure in the intersection of more than two planes. The second procedure combines this basic scheme with a second important technique: retraction etching to form a nano-structure at an edge or contour.[29,30] The pyramids fabricated following this second procedure were integrated with cantilever beams, which made it possible to handle them and place them in contact with a substrate. The contact point was studied in detail in an environmental scanning electron microscope (ESEM) to follow the formation of the water meniscus for different tip geometries.

2.1.1. Nano-Aperture at the Apex of a Pyramid

In brief, to form an aperture the material that is created in the apex of a pyramidal mold by corner lithography is first used as a mask in an inversion step, and subsequently removed. Finally, the silicon mold is removed to free the aperture. **Figure 2** illustrates the main steps and shows a SEM photograph of a typical result. The process flow starts by forming an inverted pyramidal mold by anisotropic etching using a square mask opening in a <100> silicon wafer. Next, a layer of silicon nitride is conformally deposited by low-pressure chemical vapor deposition (LPCVD) as the first step of the corner lithography. Based on the angle of the corners, this will result in a thickness $t\sqrt{3} \approx 1.73t$ in the apex ($\alpha = 70.6°$) of the pyramid and $½t\sqrt{6} \approx 1.22t$ in the ribs ($\alpha = 109.4°$).[31] Here t denotes the thickness of the silicon nitride at the flat surface. In the subsequent isotropic etching step (in HF solution), an etch distance between t and $1.22t$ results in a nanowire pyramid,[2] while a distance between $1.22t$ and $1.73t$ results in a nano-dot as is needed here (Figure 2A). These steps constitute the corner lithography. To create the freestanding pyramid containing the aperture, the next step is local oxidation of the silicon (LOCOS) using the nitride dot in the apex of the pyramid as a mask (Figure 2B), selective removal of the silicon nitride dot in phosphoric acid (Figure 2C), and finally selective removal of the silicon mold (Figure 2D). Figure 2E shows a fabricated aperture (diameter of approx. 240 nm) based on a deposited silicon nitride layer of 340 nm, a silicon oxide layer of 110 nm (on the <111>-planes), and an etch factor of 1.35 (etch distance $1.35t$). The etch factor has been chosen sufficiently above the lower limit of 1.22 to anticipate for possible wafer scale non-uniformities. A detailed study on the issue of uniformity of corner lithography will be reported elsewhere. It shows that non-uniformities in the silicon nitride deposition and etching for a layer thickness as in the current experiment is in the order of 5%.[31] The effective etch factor therefore can vary between 1.30 and 1.40, leading to small variations in the aperture size. The size of the resulting aperture is approximately 240 nm (measured from side to side). This is in reasonable correspondence with the size of the silicon nitride dot, based on the initial layer thickness of 340 nm and an ideal corner lithography process with an etch factor of 1.35 ± 0.05. Under these assumptions the top width of the nitride dot is 200 ± 20 nm. To give an indication of the realized uniformity, we measured the aperture size across an area of 3×1 cm^2. In general the apertures can be slightly rectangular due to the fact that the original mask opening for making the mold is not a perfect square. For the smallest side we measured an average of 203 nm with a standard deviation (σ) of 33 nm. For the largest side we measured 230 nm with a σ of 61 nm. This larger σ is caused by the fact that the mask imperfection has a random character.

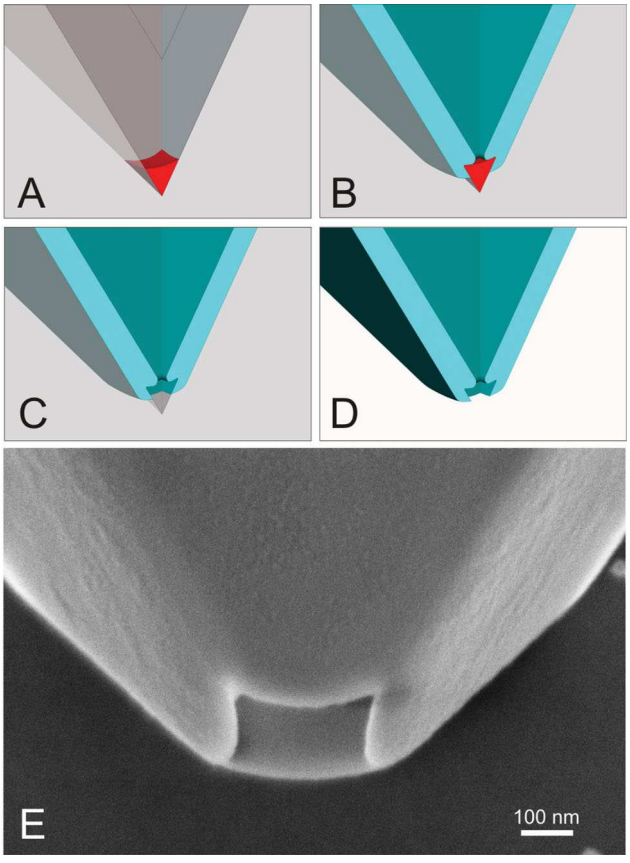

Figure 2. Fabrication scheme for aperture at the apex of the pyramid. A) Conformal deposition and isotropic thinning of silicon nitride, B) LOCOS, C) Selective removal of the silicon nitride inversion mask, D) Removal of the silicon mold, E) Resulting aperture (approx. 240 nm across).

Using the corner lithography approach it is expected that sub-100 nm apertures can be reached by reducing the initial silicon nitride and silicon oxide layer thicknesses. It is at this point important to compare our approach with the wafer scale techniques presented before. Mihalcea et al.[32] created a silicon oxide pyramidal structure in an anisotropic etch pit in a silicon mold. The combination of the oxidation retardation in the apex and an HF thinning step (when the pyramid is still in the mold) leads to a reduced thickness of the silicon oxide near the apex of a silicon oxide pyramidal structure. The apertures are opened when the mold is removed (in a KOH wet etch). The resolution of this technique is limited by the fact that the thinnest oxide is formed near and not at the apex. The smallest aperture size reported was 80 nm. Minh et al.[33] introduced a method where a silicon oxide pyramid is opened at the apex by thinning down the oxide at the convex side of the pyramid, so after removal of the mold. Important in this thinning step is the protection of the inside of the pyramid by a metal layer. This method yielded apertures as small as 25 nm. An important difference of these two reported methods with the corner lithography method is that the

DOI: 10.1002/smll.201201446

aperture is formed while the mold has already been removed. In corner lithography the aperture is formed while the structure is still in the mold, which allows for further processing of the structure formed.

2.1.2. Controllable Apertures at the Side of a Pyramid

The aim of this experiment was to create a pyramid with apertures close to the tip. Fabrication starts with KOH etching to form a pyramidal mold in a <100> silicon wafer. Next, LPCVD silicon nitride structural material is conformally deposited, followed by LPCVD poly silicon which will act as an etching mask in later steps. A second layer of silicon nitride was conformally deposited and isotropically etched in HF to form a dot in the tip apex (corner lithography, **Figure 3**A). This remnant serves as an inversion mask in the LOCOS step (wet oxidation) of the polysilicon (Figure 3B). After removal of the silicon nitride dot, a timed retraction etching of the polysilicon follows, from the apex of the pyramid moving upward (see arrows, Figure 3C). The duration of this step determines the height of the side-apertures to be formed. In the performed experiment, a layer of 330 nm polysilicon etched laterally at a speed of 420 nm/ min. in a 5 wt% TMAH solution at 70 °C. Next the silicon oxide is removed and the free accessible first silicon nitride etched in H_3PO_4. This also is a timed etch step (etch factor 1.04) as it should leave the four silicon nitride nanowires and the tip (Figure 3D). Figure 3E shows a typical fabrication result with apertures of about 1.8 µm in height. The size and the location of the side-apertures can be tuned by the thickness of in particular the silicon nitride layers (485 nm for the first layer and 120 nm for the second layer in the current experiment) and by the poly silicon etching time (105 s in the current experiment). The cantilever beam is formed in step D using the poly silicon layer as the etch mask.

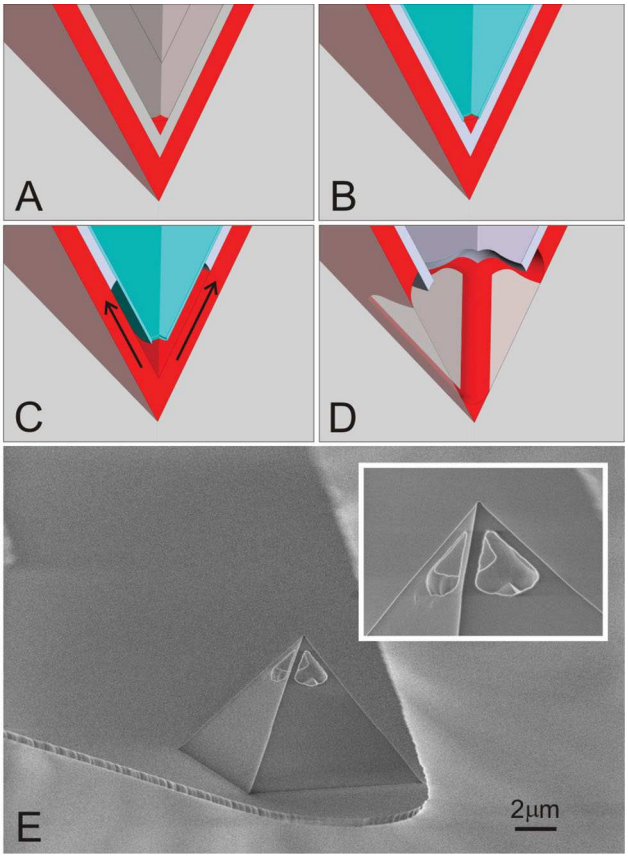

Figure 3. Fabrication of side-apertures (A-D). A) Deposition of silicon nitride, polysilicon and second silicon nitride layer. Corner lithography applied to second silicon nitride. B) LOCOS applied to the poly silicon layer. C) Removal of silicon nitride dot and subsequent retraction etching of the poly silicon. D) Removal of the silicon oxide mask, subsequent corner lithography of the first silicon nitride layer. E) Fabricated silicon nitride tip containing the side-apertures, suspended on a cantilever beam.

To test the functionality of the side-apertures, we placed a cantilever carrying a closed pyramidal surface and a cantilever carrying a pyramid with side-apertures close to each other on a piece of clean and smooth silicon wafer. Permanent adhesion (stiction) occurs between the cantilever and wafer surfaces, keeping the pyramids in contact with the substrate (**Figure 4**A, D). This substrate was then placed in the ESEM. Relative humidity (RH) level was gradually increased from 60% to 100% and SEM images from both tips made at intermediate RH levels. At the specific magnification used in the experiment we could observe a meniscus at RH levels of 95% and above. At 95% RH the meniscus size was still small and did not reach the level of the side-apertures (Figure 4B, E). At 96 and 98% the meniscus was grown to a size to reach the level of the side-apertures and a clear confinement effect could be observed (Figure 4C, F). Figure 4G shows the measured diameter of the neck of the meniscus (indicated by arrows in Figure 4C), as a function of RH. We plotted the diameter versus $-1/\ln(p/p_s)$ in which p is the water vapor pressure and p_s is the saturated vapor pressure. Following the Kelvin equation, a linear relationship is found for the closed pyramids when we assume that $p_s = 6.47$ Torr. This is very close to the tabulated $p_s = 6.55$ Torr for T = 5 °C and can reflect a small calibration error in either the temperature or the pressure sensor in the ESEM.

As expected there is no significant difference in the measured diameter between the closed pyramids and the pyramids having side apertures for 95% RH. For 98% RH (the right two points in Figure 4G) the effect of the side-apertures on the diameter of the capillary neck can be clearly be observed. This experiment shows the potential for controlling the size of the meniscus by nano-structuring of the pyramidal tip, which is for example important in nano-deposition techniques like fountain pen lithography and NADIS. However, it is only a first step as these techniques also need a guiding path for the ink from the base of the pyramid to the tip apex.

2.2. Nanowire Trapping Device

When the over-etch factor in corner lithography is in the range of 1.0–1.22, nanowires will remain in the ribs of a pyramidal mold, etched in a <100> silicon substrate.[2] Here, we integrate this pyramidal nanowire structure in a complete microfluidic filter device and demonstrate its basic functionality. **Figure 5**A-D illustrates the main fabrication steps.

small 2012,
DOI: 10.1002/smll.201201446

small NANO MICRO

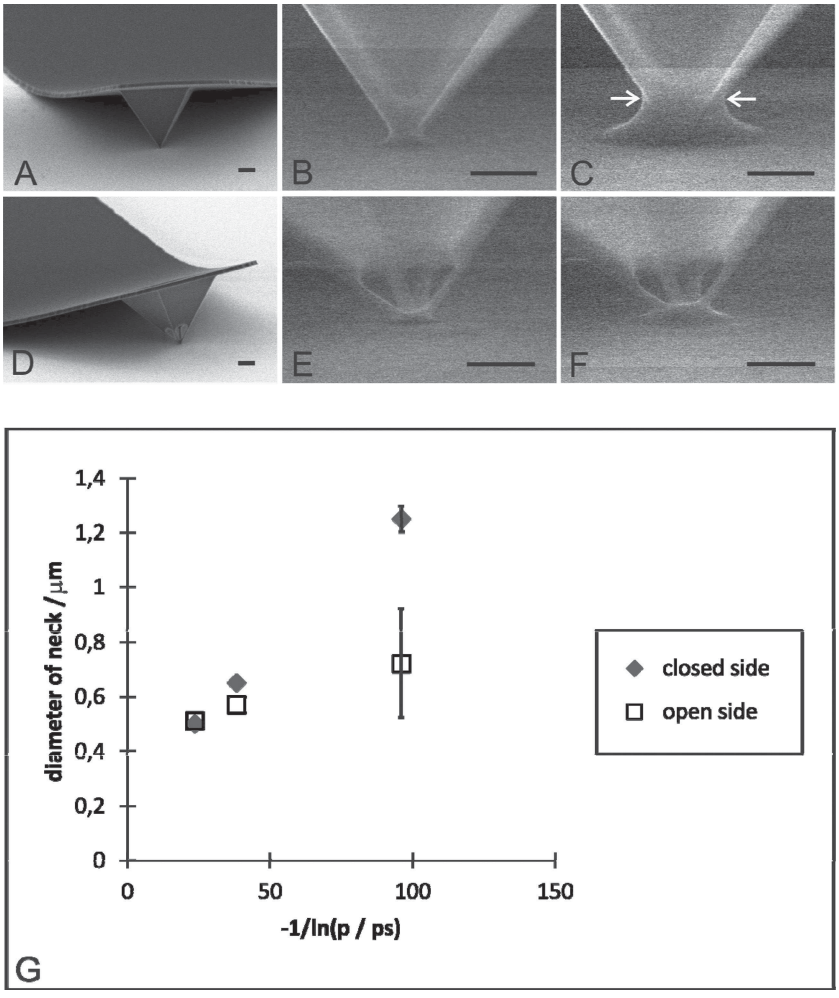

Figure 4. A solid (A), and a pyramid containing side-apertures (D) was brought in contact with a substrate (oxidized silicon wafer) by adhesion of the supporting cantilevers to the smooth substrate. B), E) ESEM photographs of the meniscus forming at the solid and perforated pyramid (95% RH), and C), F) at 98% RH. A confinement effect can be observed due to the presence of the side-apertures. The scale bars represent a 1 µm distance. Quantitatively, the graph (G) shows the measured diameter of the capillary neck for the solid pyramids (diamonds) and the pyramids having side apertures (squares). The deviation from the linear trend due to the confinement effect of the windows at 98% RH is significant. The error bars are indicative for the min-max errors in "closed side" neck diameters (small error), and the "open side" neck diameters (large error).

A silicon nitride layer is deposited and etched using a regular photoresist pattern of 5 µm diameter holes. The thus formed micro-patterned nitride layer is used as an etch-mask in the formation of the inverted pyramidal mold structures in silicon (wet anistropic etching in TMAH). To create the nanowire pyramid, silicon nitride is conformally deposited by LPCVD and isotropically etched in H_3PO_4 solution. In the present experiment an etch factor of 1.05 was applied. To create a fluidic interface, glass tubes (3 mm id) are fusion bonded to the membrane by melting the glass at 790 °C.[20,21]

Figure 5E shows a SEM photograph of the multi-scale assembly. To test the functionality of the trapping device it was placed in a transparent reservoir filled with DI water, on top of an inverted microscope. Approximately 5µL of bead suspension (4.5 µm diameter latex microspheres, *Polybead, Polysciences*) equivalent with 1.5×10^5 beads was deposited in the glass tube by careful pipetting. Next, 0.2 mL DI water was added to create a water level approximately 1 cm above the level in the reservoir. The created pressure difference was sufficient to induce a flow through the membrane and to force beads into the nanowire pyramids. **Figure 6**A shows optical microscope images taken at 100 s time interval, showing bead trapping events. Figures 6B,C show scanning electron microscope (SEM) photographs of trapped beads after drying of the structure. An important parameter is the under-etching of the silicon nitride mask layer during the formation of the pyramidal pit. It determines the size of the hole in the membrane with respect to the size of the triangular openings in the wire frame. In the current experiments we used 25 wt% TMAH at 75 °C to form the pyramidal pits in the silicon mold. This etchant has an etch rate of 16 nm/min in the <111> direction.

The device is ideally suited for trapping living cells in a relative open environment, allowing subsequently for techniques like perfusion, electroporation, patch clamping, and fluorescent microcopy. Primary bovine articular chondrocytes were successfully seeded following the procedure of **Figure 7**A. As can be observed in Figure 7B-E we were able to obtain a good cell seeding efficiency. In most cases almost all cells could be trapped in the pyramid shaped nanowires. When trying to maximize the seeding density, we obtained about 80% trapping coverage while inserting just enough cells for a theoretical 100% trapping coverage. We usually used a lesser number of cells for seeding than the total number of pyramids present in one array, and then observed that occasionally a few cells were not captured. Subsequently, cells were cultured for up to 48 hours and we observed that they retained a round morphology. Interestingly, within 2 hours after seeding filopodia-like structures could be seen which were anchoring the cells to the pyramids (Figure 7C). During prolonged culture these filopodia-like structures increased in quantity and started to bridge between individual pyramids. These fibrous structures resemble extra cellular matrix proteins as described by others during more prolonged cultures in specific tissue engineering studies[34] of chondrocytes for the formation of cartilage. During prolonged culture, individual cells were neatly kept in a predefined pattern and spacing showing that these nanowire arrays can be a feasible tool for studying single cells on a large scale in 2D while maintaining a more natural 3D phenotype. It is generally known that chondrocytes dedifferentiate into cells with a fibroblast like appearance when cultured on a standard 2D tissue culture plastic surface. Chondrocytes are generally embedded in

DOI: 10.1002/smll.201201446

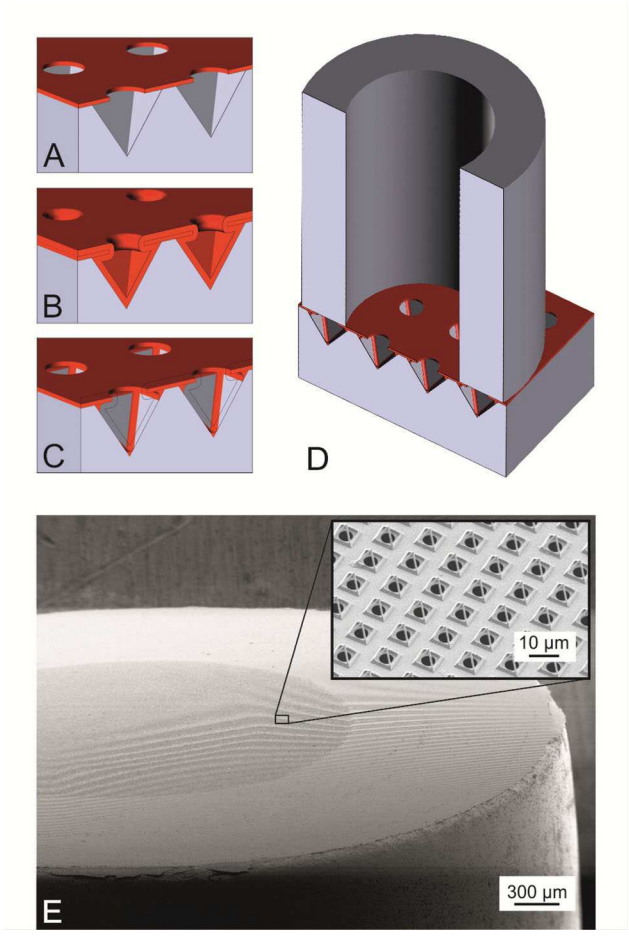

Figure 5. Fabrication scheme of nano-wire trapping device. A) Patterning of silicon nitride mask layer and anisotropic etching of inverted pyramids. B) Conformal deposition of structural silicon nitride layer. C) Isotropic back etching of the silicon nitride. D) Fusion bonding of a glass tube for interfacing. E) SEM photo of the resulting structure, looking at the filter membrane.

a vast majority of extra cellular matrix and therefore are generally believed to benefit from a three dimensional environment for retaining their natural chondrocyte phenotype.[36–40] In contrast the pyramid arrays are able to retain chondrocytes with a more rounded phenotype resembling their native phenotype. Several authors have shown the importance of cell shape and attachment for the preservation of, or differentiation into a specific phenotype. Macbeath et al. have shown that if the area a mesenchymal stem cells can adhere to is severely constrained these cells tend to display an adipocyte phenotype, while if these areas are large enough they differentiate into an osteoblast like phenotype.[35] The use of 3D corner lithography allows for the creation of 2D cell culture devices containing individual 3D cages for the entrapment of cells in a 3D microenvironment in a controllable and reproducible manner.

3. Conclusion

In conclusion we demonstrated the batch-wise fabrication of sub-micron features (apertures and wires) by a new 3D nano-patterning technique and their integration into functional fluidic devices. We demonstrated the basic functionality of the side-apertures in confining the water meniscus grown in the contact zone of the pyramidal tip. Arrays of nanowire pyramids were successfully integrated in a complete microfluidic filter device, and the trapping of micro-beads was demonstrated. Individual bovine primary chondrocytes were successfully cultured in an array of pyramids, while retaining a 3D morphology comparable to their native phenotype. In addition, we observed filopodia-like structures and protein-like deposits produced by these cells suggesting the onset of ECM formation starting already 2 h after initial cell seeding.

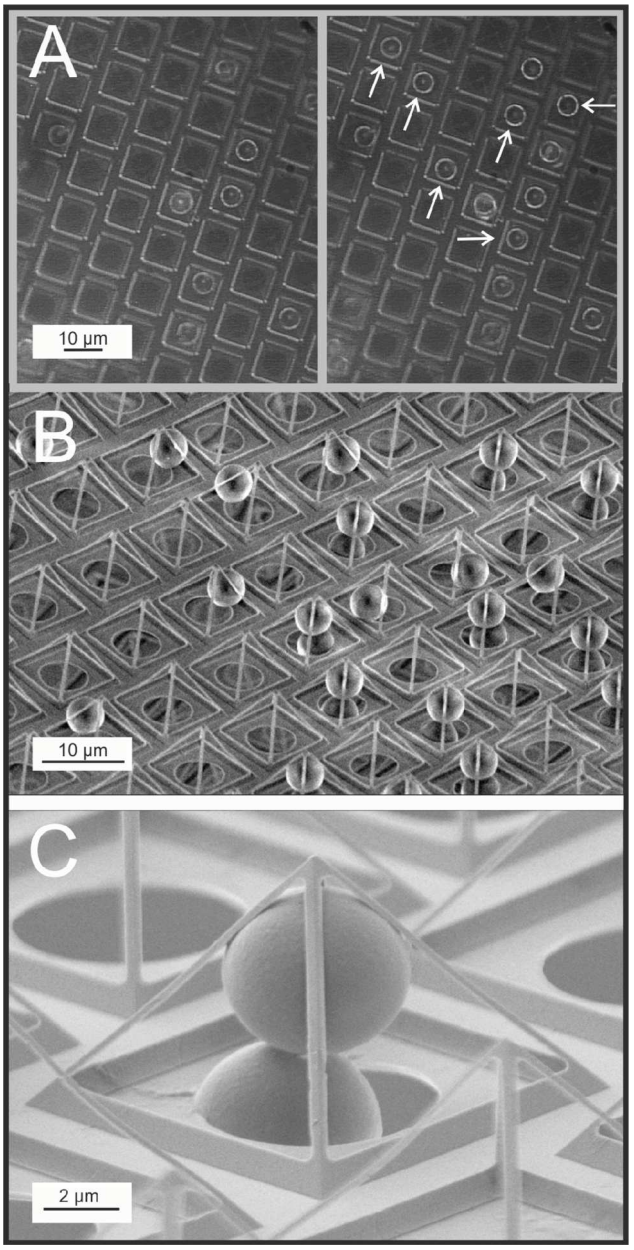

Figure 6. A) Optical microscope images of the bead trapping experiments. The arrows indicate the beads there are trapped in the 100 s time intervals. B,C) SEM photographs of trapped beads after drying of the device.

small 2012,
DOI: 10.1002/smll.201201446

NANO MICRO small

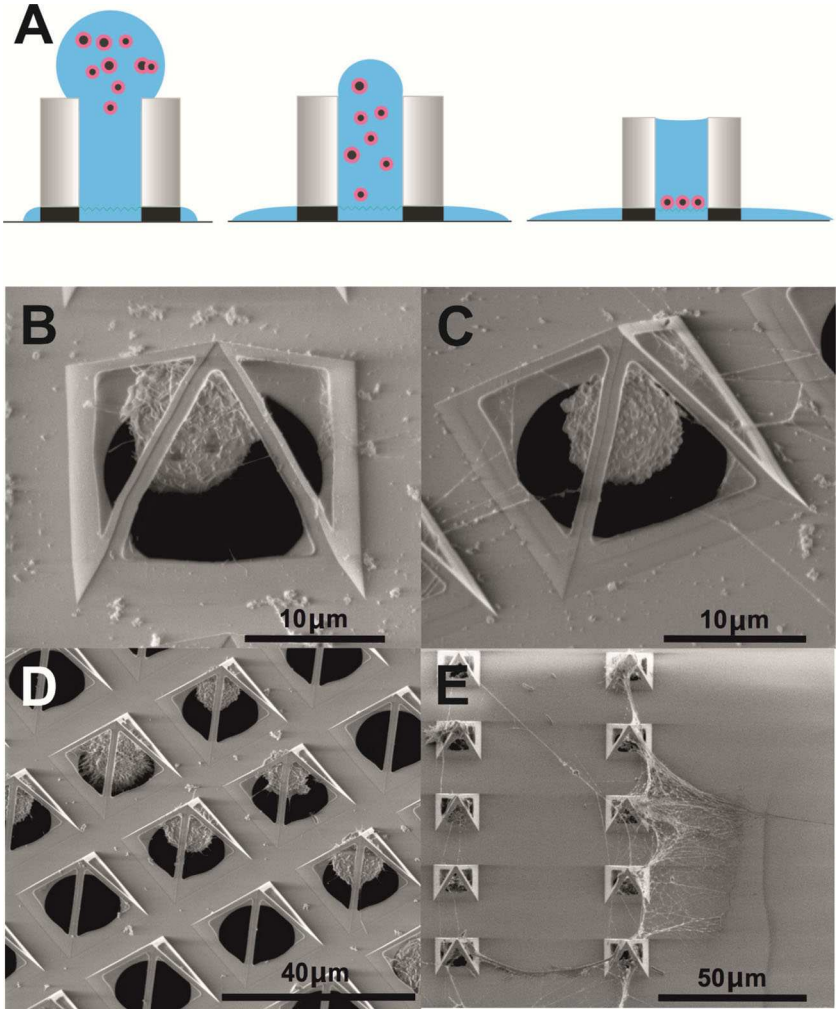

Figure 7. Seeding procedure and culturing results. A) Schematic of cell seeding, cells in suspension were added in a droplet on top of the borosilicate tubes after which they settle in individual nanowire pyramids. Flow is induced by a combination of surface tension and gravitational forces. After applying the cell suspension, additional droplets (3–4) of cell culture medium maintains the downward flow directing individual cells into the pyramids. B) Primary bovine chondrocytes 1 h and C) 2 h after seeding. Chondrocytes can be seen adhering to the ribs of the pyramid shaped nanowires while maintaining their rounded morphology. D) 24 and E) 48 h after seeding filopodia-like structures and protrusions can be seen extending through, and bridging in between the cages.

Future work will focus on using the tool to study behavior of several different primary cell types and the influence of nanowire pyramid cultures on (stem) cell differentiation and adhesion. In device fabrication we will work on further down-scaling of the corner lithography. We will expand the use of the technique in making functional nanostructures in other domains, such as thermal, mechanical, and magnetic domains.

4. Experimental Section

Nano-Aperture Fabrication: First a 100 nm silicon oxide mask layer is grown by wet thermal oxidation at 900 °C. A mask pattern containing 5 × 5 μm^2 squares was applied by standard photolithography. After patterning the mask layer in buffered HF solution, a 1% HF dip was applied for 1 minute to remove native oxide just before wet etching of the silicon. Pyramidal pits were etched into the silicon by KOH solution (25 wt%, at 75 °C) for 15 min. Samples were cleaned in RCA2 solution ($HCl:H_2O_2:H_2O$ = 1:1:5, 80 °C) and HNO_3. A 1% HF dip (1 minute) was applied to remove native oxide prior to depositing a conformal low stress film of silicon-rich silicon nitride (SiRN) layer of 340 nm by LPCVD (200 mTorr, 850 °C, SiH_2Cl_2: NH_3 flow = 3: 1). The SiRN layer was etched isotropically in H_3PO_4 solution (85 wt%, 180 °C) for 102 min to remove a thickness of 1.35 times the deposited layer thickness. This leaves a dot of approx. 200 nm across in the apex of the pyramid. The exact etch rate was checked using a dummy wafer containing the same deposited thickness of SiRN. An inversion step was carried out by LOCOS using the silicon nitride dot as the inversion mask (30 min. wet oxidation at 950 °C), resulting in a silicon oxide layer of 110 nm (on the <111>-planes). To open the aperture at the apex the SiRN dots were removed in H_3PO_4 solution (36 min) after a 1 min HF etching step (1% HF) to remove the silicon oxi-nitride formed in the LOCOS step. These steps are done in presence of a dummy wafer to check the annealed SiRN etch rate (the etch rate in H_3PO_4 is typically 30% reduced after the oxidation step). Finally, to release the pyramids the wafer was broken and the silicon etched from the side for 20 min in a TMAH solution (25 wt%, at 75 °C).

Side-Aperture Fabrication: A 120 nm SiRN-layer was deposited on a 100 mm <100> silicon wafer using LPCVD and patterned by reactive ion etching (RIE, Electrotech, Plasmafab 310–340) using a resist mask with 5 µm holes and the following etch parameters: 10 °C electrode temp., 25 sccm CHF_3 flow, 5 sccm O_2 flow, 10 mTorr pressure, 75 W power. After stripping the photoresist, pyramidal holes were etched in a KOH solution (25 wt%, 75 °C) after which the wafer was cleaned in RCA solution. Tip sharpening of the mold was achieved by wet oxidation of the silicon mold (at 1000 °C) after stripping the silicon nitride mask in 50% HF for 45 min. To create the structure in Figure 3A a layer of 500 nm silicon nitride, a layer of 330 nm poly silicon and a layer of 120 silicon nitride were subsequently deposited by LPCVD (an HF dip proceeding the last deposition step). Corner lithography was performed to the last layer using HF 50% (3.6 nm/min etch rate). An etch factor of 1.27 was used, calibrated by etching of a dummy wafer in parallel. Inversion of the created dot in the apex was achieved by local oxidation of the poly silicon (LOCOS) (wet oxidation at 900 °C for 10 min, approx. 50 nm). To create the cantilever, the LOCOS oxide is patterned by standard photo-lithography followed by 150 s (buffered) BHF etching and stripping of the photo resist. This LOCOS mask is later transferred into the underlying poly silicon and then into the first silicon nitride. To open the poly silicon at the tip apex, the

DOI: 10.1002/smll.201201446

remaining silicon nitride is removed in H_3PO_4 solution (85 wt%, 180 °C). To reach to the situation of Figure 3C the poly silicon is etched for 105 s in a 5% TMAH solution (70 °C), at a lateral etch rate of 486 nm/min (plain layer 700 nm/min). Finally, the LOCOS layer was stripped in BHF, to reveal the poly silicon mask for patterning of the remaining silicon nitride layer (500 nm). Patterning was done by H_3PO_4 etching (85 wt%, 180 °C) for 127 min (etch factor 1.04) to reach to the situation of Figure 3D. The devices were completed by removing the poly silicon mask in 5% TMAH solution (70 °C) after an HF dip and anodic bonding of the silicon wafer to a pre-diced pyrex wafer (450 °C, 800 V). Prior to bonding an 8 nm LPCVD oxide layer was deposited to avoid bubble formation during anodic bonding. After dicing from the backside of the glass wafer the silicon nitride devices were etched free by KOH etching (25 wt% at 70 °C for 8 h) followed by RCA cleaning and stripping of the sharpening silicon oxide in BHF for 7 min. This completed the devices up to the stage that they can be released by breaking–out the samples.

ESEM Experiments: A cantilever carrying a solid pyramid and a cantilever carrying a pyramid having side-apertures were placed close to each other on a piece of clean and smooth silicon wafer. Permanent adhesion (stiction) occurs between the cantilever and wafer surfaces, keeping the pyramids in contact with the substrate. The substrate was then placed in the ESEM (FEI/Philips XL30 Feg). Experiments were carried out at a fixed chuck temperature of 5 °C. The relative humidity (RH) was regulated by varying the water vapor pressure from 3.9 to 6.4 Torr in six steps, corresponding with RH levels increasing from 60% to 98%. At each RH level an ESEM image was taken from both tips at the same magnification.

Nanowire Trapping Device Fabrication: A 500 nm silicon-rich silicon nitride layer (SiRN) is deposited on a 100 mm <100> silicon wafer using Low-Pressure Chemical Vapor Deposition (LPCVD) and patterned by reactive ion etching (RIE) using a resist mask with 5 µm holes. After stripping the resist in an oxygen plasma and native oxide removal by 1%HF, pyramidal pits bounded by <111> planes are etched through these holes in 25% TMAH at 75°. (Etchrate <100> planes = 300 nm/min, etchrate <111> planes = 16 nm/min). Etching time of 97 min. gives an undercut of the SiRN mask holes of 1.9 µm. Next, the structures are conformally coated by a LPCVD SiRN layer of 770 nm +/–20 nm followed by isotropically thinning down in 85% H_3PO_4 at 180° leaving the nanowires in sharp concave corners. Tuning of the etching time is based on etching SiRN dummy wafers having the same thickness as the process wafers. Ellipsometric measurements (plasmos SD 2002 ellipsometer) in combination with hydrophobic surface change sets the endpoint of etching the SiRN. An over-etch factor of 1.05 was applied for compensating the non-uniformity of the SiN layer ensuring wafer scale nanowire fabrication. Backside removal of 500 nm SiRN is done using RIE (first deposited SiRN layer).

Borosilicate glass tubes (3 mm id, 6 mm od, Duran, Schott AG) are diced at 20 mm length and polished to optical grade. They are fusion bonded to the membrane by melting the glass tubes at 790 °C (30 min, ramp-up 10 °C/min, ramp-down 20 °C/min, oven: Nabertherm LH 15/12). Finally, the membrane and nanowires are released by dissolving the silicon substrate wafer in a TMAH solution (5% at 75 °C, etchrate <100> planes = 600 nm/min).

Bead Trapping Experiments: The trapping device was placed in a transparent reservoir filled with de-ionized (DI) water, on top of an inverted microscope (Leica DMI5000). The device was resting on a spacer ring and the membrane just submerged in the water. Approximately 5µL of bead suspension (4.5 µm diameter latex microspheres, Polybead, Polysciences) equivalent with 1.5×10^5 beads was deposited in the glass tube by careful pipetting. Next, 0.2 mL DI water was added to create a water level approximately 1 cm above the level in the reservoir. The created pressure difference was sufficient to induce a flow through the membrane and to force beads into the nanowire pyramids. During the experiment the membrane was observed in bright field mode, through a 40x objective (HCX PL Fluotar, NA 0.60 (Corr.)). Trapping experiments were continuously recorded by a camera (Procilica CV 1280), at a frame rate of 10 images per second.

Cell Culture and Seeding Single Cells: The initial nanowire trapping device was adapted to allow for cell entrapment and tissue culture handling. In brief the dimensions were adapted to allow for the seeding of primary bovine articular chondrocytes, (passage 3, p3). Nanowire trapping devices with a pore diameter of 16 µm and membrane rib width of 19.6 µm and 10.7 µm height were produced according to the previously mentioned micromachining method. Cryopreserved primary chondrocytes (p2) were thawed and plated at 3000 cell/cm^2 and cultured until 80% confluence during 6 days at 37 °C, 5% CO_2 using DMEM (Gibco-BRL, the Netherlands) supplemented with 10% fetal bovine serum (Sigma-Aldrich, Milwaukee, WI, USA), ascorbic acid 2-phospate (0.2 mM, Gibco-BRL, the Netherlands), non-essential amino acids (0.1 mM, Sigma-Aldrich, the Netherlands), proline (0.4 mM, Sigma-Aldrich, the Netherlands), penicillin (100 units/mL, Gibco-BRL, the Netherlands) and streptomycin (100 mg/ml, Gibco-BRL, the Netherlands). Subsequently cells were washed 2x in PBS and trypsinized and resuspened in PBS to a final stock solution of 50 cells/µL. Cells were seeded in droplets of 20 µL deposited onto a borosilicate tube, which was bonded on top of the nanowire trapping array according to the schematic in Figure 7 and using droplets of 20–30 µL. After applying the cell suspension, additional droplets (3–4) of cell culture medium maintains the downward flow directing individual cells into the pyramids. Cells were allowed to settle and attach for 2 hrs, and subsequently cultured for 24 h and 48 h. Cells were fixed afterwards using 4% paraformaldehyde and dehydrated using an increasing ethanol solution series (70 to 100%). Samples were then processed for SEM using a Balzers-CPD030 critical point dryer and gold sputter coated using a Cressington 108SE sputter coater and observed using SEM (FEI Quanta 450).

Acknowledgements

We gratefully acknowledge the stimulating discussions with Dr. Abelmann (TST group, MESA+ Institute for Nanotechnology), as well as Dr. Sarajlic (SmartTip B. V.) on corner lithography and several applications of this technique. We would like to thank Mark Smithers for taking the SEM photographs. This work was partly carried out within the FunTips project, which is supported by NWO/STW through a Vidi grant.

small 2012,
DOI: 10.1002/smll.201201446

[1] S. Reyntjens, R. Puers, *J. Micromech. Microeng.* **2001**, *11*, 287–300.
[2] E. Sarajlic, E. Berenschot, G. Krijnen, M. Elwenspoek, *Proc. 13th Int. Conf. on Solid–State Sensors, Actuators and Microsystems (Transducers '05)* **2005**, 27–29.
[3] E. Berenschot, R. Tas Niels, V. Jansen Henri, Miko Elwenspoek, *Proc. 3rd IEEE Int. Conf. On Nano/Micro Engineered and Molecular Systems* **2008**, 729–732.
[4] X. Yu, H. Zhang, J. K. Oliverio, Paul V. Braun, *Nano Lett.* **2009**, 4424–4427.
[5] R. D. Piner, J. Zhu, F. Xu, S. Hong, C. A. Mirkin, *Science* **1999**, *283*, 661–663.
[6] A. Meister, M. Liley, J. Brugger, R. Pugin, H. Heinzelmann, *Appl. Phys. Lett.* **2004**, *85*, 6260–6262.
[7] A. Meister, S. Jeney, M. Liley, T. Akiyama, U. Staufer, N. F. de Rooij, H. Heinzelmann, *Microelectr. Eng.* **2003**, *67–68*, 644–650.
[8] A. Fang, E. Dujardin, Th. Ondarçuhu, *Nano Lett.* **2006**, *6*, 2368–2374.
[9] S. Deladi, N. R. Tas, J. W. Berenschot, G. J. M. Krijnen, M. J. de Boer, J. H. de Boer, M. Peter, M. C. Elwenspoek, *Appl. Phys. Lett.* **2004**, *85*, 5361–5363.
[10] K.-H. Kim, N. Moldovan, H. C. Espinosa, *Small* **2005**, *1*, 632–635.
[11] P. Dörig, P. Stiefel, P. Behr, E. Sarajlic, D. Bijl, M. Gabi, J. Vörös, J. A. Vorholt, T. Zambelli, *Appl. Phys. Lett.* **2010**, *97*, 023701.
[12] S. Arscott, D. Troadec, *Appl. Phys. Lett.* **2005**, *87*, 134101.
[13] C. Dekker, *Nat. Nanotechnol.* **2007**, *2*, 209–215.
[14] D. Branton, D. W. Deamer, A. Marziali, H. Bayley, S. A. Benner, T. Butler, M. Di Ventra, S. Garaj, A. Hibbs, X. Huang, S. B. Jovanovich, P. S. Krstic, S. Lindsay, X. Sean Ling, C. H. Mastrangelo, A. Meller, J. S. Oliver, Y. V. Pershin, J. M. Ramsey, R. Riehn, G. V. Soni, V. Tabard-Cossa, M. Wanunu, M. Wiggin, J. A. Schloss, *Nat. Biotechnol.* **2008**, *26*, 1146–1153.
[15] L. Ma, S. L. Cockroft, *ChemBioChem* **2010**, *11*, 25–34.
[16] G. F. Schneider, S. W. Kowalczyk, V. E. Calado, G. Pandraud, H. W. Zandbergen, L. M. K. Vandersypen, C. Dekker, *Nano Lett.* **2010**, *10*, 3163–3167.
[17] S. Kuiper, C. J. M. van Rijn, W. Nijdam, M. C. Elwenspoek, *J. Membr. Sc.* **1998**, *150*, 1–8.
[18] H. D. Tong, H. V. Jansen, V. J. Gadgil, C. G. Bostan, E. Berenschot, C. J. M. van Rijn, M. Elwenspoek, *Nano Lett.* **2004**, *4*, 283–287.
[19] J. K. Holt, H. G. Park, Y. Wang, M. Stadermann, A. B. Artyukhin, C. P. Grigoropoulos, A. Noy, O. Bakajin, *Science* **2006**, *312*, 1034–1037.
[20] B. Mogulkoc, H. V. Jansen, J. W. Berenschot, H. J. M. Ter Brake, K. M. Knowles, M. C. Elwenspoek, *J. Micromech. Microeng.* **2009**, *19*, 085027.
[21] S. Unnikrishnan, H. Jansen, E. Berenschot, B. Mogulkoc, M. Elwenspoek, *Lab Chip* **2009**, *9*, 1966–1969.
[22] P. V. Schwartz, *Langmuir* **2002**, *18*, 4041–4046.
[23] H. Andersson, A. van den Berg, *Sens. Act. B* **2003**, *92*, 315–325.
[24] P. Wilding, L. J. Kricka, J. Cheng, G. Hvichia, M. A. Shoffner, P. Fortina, *Anal. Biochem.* **1998**, *257*, 95–100.
[25] M. Yang, C-W. Li, J. Yang, *Anal. Chem.* **2002**, *74*, 3991–4001.
[26] H. Andersson, W. Van der Wijngaart, P. Enoksson, G. Stemme, *Sens. Act. B* **2000**, *67*, 203–208.
[27] Y. Huang, B. Rubinsky, *Sens. Act.* **2002**, *89*, 242–249.
[28] C. L. Randall, Y. V. Kalinin, M. Jamal, T. Manohar, D. H. Gracias, *Lab on Chip* **2011**, *11*, 127–131.
[29] B. D. Gates, Q. Xu, M. Stewart, D. Ryan, C. G. Willson, G. M. Whitesides, *Chem. Rev.* **2005**, *105*, 1171–1196.
[30] Y. Zhao, E. Berenschot, H. Jansen, N. Tas, J. Huskens, M. Elwenspoek, *Microelectr. Eng.* **2009**, *86*, 832–836.
[31] N. Burouni, E. Berenschot, M. Elwenspoek, N. Tas, *Proc. 6th IEEE Int. Conf. On Nano/Micro Engineered and Molecular Systems* **2011**, 940–943.
[32] C. Mihalcea, A. Vollkopf, E. Oesterschulze, *J. Electrochem. Soc.* **2000**, *147*, 1970–1972.
[33] P. N. Minh, T. Ono, M. Esashi, *APL* **1999**, *75*, 4076–4078.
[34] L. Moroni, R. Schotel, D. Hamann, J. R. de Wijn, C. A. van Blitterswijk, *Adv. Funct. Mat.* **2008**, *18*, 53–60.
[35] R. McBeath, D. N. Pirone, C. M. Nelson, K. Bhadriraju, C. S. Chen, S. Christopher, *Develop. Cell* **2004**, *6*, 483–495.
[36] R. Cancedda, F. Descalzi-Cancedda, P. Castagnola, *Int. Rev. Cytol.* **1995**,*159*, 265–358.
[37] K. von der Mark, V. Gauss, H. von der Mark, P. Müller, *Nature* **1977**, *267*, 531–532.
[38] M. D. Buschmann, Y. A. Gluzband, A. J. Grodzinsky, J. H. Kimura, E. B. Hunziker, *J. Orthop. Res.* **1992**, *10*, 745–758.
[39] J. Bonaventure, N. Kadhom, L. Cohen-Solal, K. H. Ng, J. Bourguignon, C. Lasselin, P. Freisinger, *Exp. Cell Res.* **1994**, *212*, 97–104.
[40] D. A. Lee, T. Reisler, D. L. Bader, *Acta Orthop. Scand.* **2003**, *74*, 6–15.

Received: June 26, 2012
Published online: